


Diverse PSMA expression in primary prostate cancer: reason for negative [^{68}Ga]Ga-PSMA PET/CT scans? Immunohistochemical validation in 40 surgical specimens

Wojciech Cytawa^{1,2}  · Stefan Kircher³ · Hubert Kübler⁴ · Rudolf A. Werner¹ · Simon Weber¹ · Philipp Hartrampf¹ · Tomasz Bandurski⁵ · Piotr Lass² · Wojciech Połom⁶ · Marcin Matuszewski⁶ · Hans-Jürgen Wester⁷ · Constantin Lapa⁸ · Andreas Rosenwald³ · Anna Katharina Seitz⁴ · Andreas K. Buck¹

Abstract

Purpose The purpose of this study was to immunohistochemically validate the primary tumor PSMA expression in prostate cancer (PCa) patients imaged with [^{68}Ga]Ga-PSMA PET/CT prior to surgery, with special consideration of PET-negative cases.

Methods The study included 40 men with newly diagnosed treatment-naïve PCa imaged with [^{68}Ga]Ga-PSMA I&T PET/CT as part of the diagnostic work-up prior to radical prostatectomy. All primary tumors were routinely stained with H&E. In addition, immunohistochemical staining of PSMA was performed and the immunoreactive score (IRS) was computed as semiquantitative measure. Subsequently, imaging findings were correlated to histopathologic results.

Results Eighty-three percent (33/40) of patients presented focal uptake of [^{68}Ga]Ga-PSMA I&T in the primary tumor in at least one prostate lobe. Among PSMA-PET positive patients, one-third had lymph node metastases (LNM) detected by post-operative histopathology, while in PET negative patients, only 1 out of 7 presented with regional LN involvement; PSMA-avid distant lesions, predominantly in bones, were observed in 15% and 0% of patients, respectively.

The median IRS classification of PSMA expression in tumor tissue was 2 (range, 1–3) both in PSMA-PET positive and negative prostate lobes, with significantly different interquartile range: 2–3 vs. 2–2, respectively ($p = 0.03$). The median volume of PSMA-PET positive tumors was 5.4 mL (0.2–32.9) as compared to 1.6 mL (0.3–18.3) of PET-negative tumors ($p < 0.001$). There was a significant but weak correlation between SUV_{max} and percentage of PSMA-positive tumor cells ($r = 0.46$, $p < 0.001$). A total of 35/44 (~80%) lobes were positive in PSMA-PET imaging, when a cut-off percentage of PSMA-positive cells was $\geq 90\%$, while 19/36 (~53%) lobes with $< 90\%$ PSMA-positive cells were PSMA-PET negative.

Conclusion Positive [^{68}Ga]Ga-PSMA I&T PET/CT scan of primary tumor of PCa results from a combination of factors, such as homogeneity and intensity of PSMA expression, tumor volume and grade, with a cutoff value of $\geq 90\%$ PSMA-positive cells strongly determining PET-positivity. Focal accumulation of [^{68}Ga]Ga-PSMA in the primary tumor may correlate positively with aggressiveness of prostate cancer, harboring higher risk of regional LN involvement and distant metastatic spread.

Keywords Prostate cancer · PSMA · PET/CT · Immunohistochemistry

This article is part of the Topical Collection on Oncology - Genitourinary

Wojciech Cytawa and Stefan Kircher contributed equally to the manuscript. Anna Katharina Seitz and Andreas K. Buck shared the last authorship.

Piotr Lass is deceased.

✉ Wojciech Cytawa
wcytawa@gumed.edu.pl

Extended author information available on the last page of the article

Introduction

Worldwide, prostate cancer (PCa) is the second most common malignant tumor in men with more than 1,400,000 new cases in 2020 [1]. In addition to clinical, biochemical, and histological work-up, optimal patient management requires accurate staging of the disease. This is most often provided by non-invasive imaging modalities, such as transrectal ultrasonography (TRUS), computed tomography (CT), magnetic resonance imaging (MRI), and bone scan.

Recently, positron emission tomography/CT (PET/CT) using various gallium-68- and fluorine-18-labelled ligands of the prostate-specific membrane antigen (PSMA) has been successfully introduced in this clinical setting. PSMA is a membrane bound receptor highly expressed on the surface of PCa cells with only low-level expression in normal prostate [2]. The ligands are small molecule compounds based on the chemical motif *glutamate-urea-lysine* which present high binding affinity to the PSMA receptor and can act as excellent target vectors of PCa [3]. However, despite very high sensitivity and specificity of PSMA-PET for detecting disease foci reaching 80–90% [4], there is still up to 20% of patients presenting inadequate PSMA expression in PCa lesions at imaging, thus making PSMA-guided theranostics unreliable in a subcohort of patients [5]. While much data has been published on increasing PSMA expression with tumor dedifferentiation particularly in hormone-refractory and metastatic PCa [6], there are very few papers explaining the lack of PSMA expression in a significant proportion of individuals.

The aim of this study was to immunohistochemically validate PSMA expression in PCa patients imaged with [^{68}Ga] Ga-PSMA PET/CT performed before radical prostatectomy (RP) with extended pelvic lymph node dissection (ePLND). Special attention was paid to the PSMA-negative cases, i.e., patients without focal uptake in the primary tumor at pre-operative PSMA PET. Another aim was to compare survival outcomes in PSMA-PET positive and negative patients after definitive treatment.

Material and methods

Patient recruitment

Between October 2016 and August 2018, 40 patients with newly-diagnosed PCa, 20 with intermediate- and 20 with high-risk disease according to D'Amico classification [7], underwent radical prostatectomy with ePLND (recommended if the estimated risk of lymph node metastases exceeds 5% according to the European Association of Urology (EAU) [8]). For the purpose of primary staging of the disease before surgery, all the patients were imaged with [^{68}Ga] Ga-PSMA I&T PET/CT. The cohort was partially described in our previous publication [9].

[^{68}Ga] Ga-PSMA was administered for clinical work-up in compliance with §37 of the Declaration of Helsinki and the German Medicinal Products Act, §13 2b AMG, and in accordance with the responsible regulatory body (Regierung von Oberfranken, Bavaria, Germany). All patients gave written informed consent to undergo [^{68}Ga] Ga-PSMA PET/CT imaging.

Pre-operative imaging

Preparation of [^{68}Ga] Ga-PSMA I&T

[^{68}Ga] Ga-PSMA was prepared using a cassette-based radiotracer synthesis module (GRP Scintomics, Fürstfeldbruck, Germany) according to the method established in our department which has been outlined before [9]. Briefly, the eluate ([^{68}Ga] Ga $^{3+}$ in 0.1 M HCl) of a [^{68}Ge] Ge/[^{68}Ga] Ga generator (GalliaPharm®, Eckert & Ziegler AG, Berlin, Germany) was transferred to a cation exchange cartridge, eluted with 5 N NaCl, added to a solution of 20 μg PSMA I&T (Scintomics, Fürstfeldbruck, Germany) in HEPES-buffer and heated for 6 min at 125 °C. The product was immobilized on a SepPak C18-cartridge, washed with water, and eluted with ethanol/water 50/50. The eluate was passed through a sterile filter (0.22 μm) into a sterile vial and diluted with phosphate buffer solution to a total volume of 15 mL. Radiochemical purity was determined by gradient high performance liquid chromatography and thin-layer chromatography. Additionally, the product was also tested for ethanol content, pH, radionuclide purity, sterility, and endotoxins.

Acquisition parameters of [^{68}Ga] Ga-PSMA PET/CT

The patients were imaged using a 64-slice PET/CT scanner (Siemens Biograph mCT 64, Siemens Healthineers, Erlangen, Germany) after injection of a mean activity of [^{68}Ga] Ga-PSMA of 139 ± 22 MBq (range, 88–175 MBq). The mean uptake period was 65 ± 7 min. PET emission data were acquired with 6–8 bed positions (adjusted to patient's height) from the base of the skull to the proximal thighs (2–3 min emission time per bed position). Subsequently, a monophasic full-dose CT scan was performed after injection of i.v. contrast (Imeron 350, weight-adapted, 1 mL/kg body weight) and ingestion of oral contrast (30mL Peritran in 1 L of water). The following acquisition parameters were applied: CARE Dose 4D, 160 mAs, 120 kV, 512×512 matrix, 5-mm slice thickness, slice collimation 64×0.6 mm, pitch index: 1.4. All PET images were reconstructed with an iterative algorithm (HD-PET, 24 subsets, 3 iterations, Gaussian filtering: 5 mm, $171 \times 200 \times 200$ matrix, axial resolution: 5 mm, in-plane resolution: 4.07×4.07 mm 2) using dedicated manufacturer software (syngo MI.PET/CT, Siemens Healthineers, Erlangen, Germany). No adverse reactions were observed after administration of radiopharmaceutical and contrast media.

Histopathological examination

All 40 primary tumors as well as surrounding normal prostate tissue and pelvic lymph nodes resected during RP were assessed pathologically. In a first step, representative

sections from the right and left prostate lobe were stained with *Hematoxylin and Eosin* (H&E) to establish the diagnosis of prostate cancer and potential lymph node involvement. Subsequently, from each lobe, one representative slide with the largest tumor burden was chosen for immunohistochemical (IHC) validation of PSMA expression. For this purpose, 4- μ m-thick, formalin-fixed, and paraffin-embedded tissue sections were prepared for IHC staining with the use of a PSMA-specific monoclonal antibody (clone 3E6, Dako, Hamburg, Germany). The sections were first mounted on Superfrost Plus slides (Fisher Scientific, Hampton, USA), then dewaxed and rehydrated to water by a series of graduated ethanol washes, and then incubated in a microwave oven (800 W) using ethylenediaminetetraacetic acid buffer (10 mmol/L; pH 8.0). After that, the sections were incubated with monoclonal anti-PSMA for 1 h at room temperature. Finally, the sections were counterstained with hematoxylin. The intensity of PSMA staining within tumor foci was reported in a 4-point scale (0, no color reaction; 1, mild; 2, moderate; 3, intense reaction) and multiplied by a factor (0–4) representing the percentage of positively stained cells (0, no positive cells; 1, <10%; 2, 10–50%; 3, 51–80%; 4, >80% positive cells) to obtain the immunoreactive score (IRS) (0–1, negative; 2–3, mild; 4–8, moderate; 9–12, strongly positive). IRS was then transposed to IRS classification (0, negative; 1, positive, weak; 2, positive, mild; 3, positive, strong expression), according to the method adopted from Kaemmerer et al. for somatostatin receptor staining in neuroendocrine tumors [10]. Apart from that, the intensity and percentage of PSMA positively stained cells were also reported for normal prostate (NP) tissue found in both lobes of prostate glands. The evaluation of the stains was performed by 3 independent investigators (WC, SK, SW).

Image analysis

All PET/CT scans were carefully analyzed by two board certified nuclear medicine specialists with more than 10 years of experience (WC, CL) and one nuclear medicine physician after 2 years of training (PH). Readers were aware of physiology and potential pitfalls of PSMA PET/CT imaging [11]. In case of disagreement, mutual re-evaluation of images was performed to achieve consensus. Images of the primary tumors were interpreted according to recently published PSMA-RADS Version 1.0 criteria [12]. In brief, for evaluation of the malignant primary, focal activity within the prostate gland significantly above the surrounding background level (apart from physiological activity in urethra), without pre-defined threshold values, was considered PSMA-positive. Within the pelvic lymphatic drainage areas, LNs with focally increased uptake were reported as positive (N1, according to PROMISE criteria proposed by Eiber et al. [13]). Retroperitoneally or higher located positive LNs

indicated (extrapelvic) M1a disease. PSMA-avid skeletal lesions suggesting bone metastases (BM, M1b) or other PSMA-positive visceral lesions suspicious of metastases (M1c) were reported when present.

Correlation of imaging findings with histopathology

The tumor burden, i.e., the percentage of involved tissue in both lobes of resected prostate glands was estimated during microscopic evaluation of H&E stained slices. The prostate gland dimensions — width (W), length (L), and height (H) — were obtained from computer tomography (CT) images, which allowed calculation of the volume of prostate gland according to the formula used in magnetic resonance imaging [14]:

$$\text{Prostate Volume} = W \times L \times H \times 0.523\text{mL}$$

Hence, the tumor volume (TV) in each lobe was estimated by multiplying the percent of lobular involvement by the lobe volume being a half the prostate volume. The calculation of TV was of special importance because of potential risk of partial volume effect (PVE) in small lesions which is possibly responsible for underestimation of tracer uptake [15].

The intensity of [^{68}Ga]Ga-PSMA uptake expressed as maximum standardized uptake value (SUV_{max}) was measured on PET/CT images, separately for each prostate lobe and correlated with the respective values of TV and IRS. Tracer uptake within each prostate lobe was visually defined as focal (PSMA-positive) or non focal (PSMA-negative).

The IHC validation of LNs with focal and non-focal [^{68}Ga]Ga-PSMA uptake included assessment of percentage and intensity of PSMA staining of cancerous cells.

Analysis of survival

The survival analysis was based on the primary outcome which was as follows:

1. Biochemical progression after treatment with curative intent, defined as two consecutive PSA rises > 0.2 ng/mL after RP or the rise of PSA > 2 ng/mL above the nadir after adjuvant radiotherapy, or
2. Commencement of salvage radiotherapy or androgen deprivation therapy as a result of radiographic or clinical progression, in the absence of biochemical progression.

Statistical analysis

The statistical analysis was performed with Statistica 13.1 software (StatSoft, Kraków, Polska). The normal distribution of the variables (age, PSA levels, GSC, radioisotope activity) was verified by the Shapiro-Wilk *W* test. Normally

distributed values were described as mean \pm standard deviation (SD, range) and calculated with Student's *t*-test; values without normal distribution were described as median and range, and analyzed with Mann-Whitney *U* test. To compare three or more groups, Kruskal-Wallis test was used. Linear correlation was expressed by Pearson's correlation coefficient. Kaplan-Meier curves were used for graphical presentation of survival in PSMA-PET positive and negative patients; Cox's *F* test was used to compare survival in the two groups. In all cases, a *p*-value < 0.05 was considered statistically significant.

Results

Patient characteristics

Mean patient age at the time point of PET/CT scanning was 66 ± 7 years (range 53–78). Subjects underwent surgery after a median time interval of 14 days (2–199) after the examination. Median GSC was 7 (7–10), while median ISUP grade group was 3 (2–5). Median PSA value was 11.4 ng/mL (2–140). Twelve patients had pelvic LNM detected in post-operative H&E staining and 5 patients presented with M+ disease on PSMA PET/CT, with distant lesions located predominantly in bone structures (M1b), of whom one patient had also a single PSMA-avid para-aortic LN (M1a). Detailed patients' characteristics are presented in Table 1.

PSMA PET findings in primary tumors

Eighty-three percent (33/40 patients) presented with focal uptake of [^{68}Ga]Ga-PSMA in the primary tumor (rated

PSMA-positive) in at least one prostatic lobe, with 48% (19/40) showing bilateral focal uptake. Overall, focally increased [^{68}Ga]Ga-PSMA accumulation could be detected in 65% (52/80) of prostatic lobes. In 17% (7/40) patients, mild diffuse [^{68}Ga]Ga-PSMA uptake pattern was observed but no focal lesions; consequently, PSMA PET was interpreted as negative.

The median SUV_{max} of PSMA-positive lobes was 12.8 (4.5–54.1) and was significantly higher than median SUV_{max} of PSMA-negative lobes (4.3; 2.7–6.2, Mann-Whitney *U* test, *p* < 0.001; Fig. 1).

IHC validation of PSMA expression and correlation to [^{68}Ga]Ga-PSMA uptake

Primary tumors

In all prostatic lobes (80/80), post-operative histopathological examination confirmed the presence of PCa. Median GSC in PSMA-positive (52/80) and negative lobes (28/80) was 7 (7–10) and 7 (7–10), respectively, with significantly different interquartile range (IQR): 7–9 vs. 7–7, respectively (*p* = 0.03, Mann-Whitney *U* test).

In the 52 lobes presenting focal [^{68}Ga]Ga-PSMA uptake as compared to non-focal prostate lobes, the immunoreactive score (IRS) was 8 (3–12, IQR 6–12) vs. 7 (2–12, IQR 4–8), respectively (*p* = 0.02, Mann-Whitney *U* test). The IRS classification in both groups was 2 (1–3), with significantly different IQR: 2–3 vs. 2–2, respectively (*p* = 0.03, Mann-Whitney *U* test). The mean IRS classification values are presented in Fig. 2.

Table 1 Detailed patients' characteristics

Mean age in years	66 ± 7 (53–78)
Median delay between PSMA PET/CT and operation (RP + ePLND) in days	14 (2–199)
Gleason Score	7 (<i>n</i> = 25) 8 (<i>n</i> = 4) 9 (<i>n</i> = 10) 10 (<i>n</i> = 1)
PSA (ng/mL)	≤ 1.0 (<i>n</i> = 0) 1.1–2.0 (<i>n</i> = 1) 2.1–5.0 (<i>n</i> = 2) 5.1–10.0 (<i>n</i> = 12) 10.1–20.0 (<i>n</i> = 14) > 20.0 (<i>n</i> = 11)
Risk group *	Intermediate-risk (<i>n</i> = 20) High-risk (<i>n</i> = 20)

* According to D'Amico classification [7]. PSMA, prostate-specific membrane antigen; RP, radical prostatectomy; ePLND, extended pelvic lymph node dissection; PSA, prostate-specific antigen serum level

Fig. 1 Comparison of intensity of [^{68}Ga]Ga-PSMA uptake in the primary tumor of prostate cancer in lobes with focal accumulation (PSMA-positive) and without focal accumulation (PSMA-negative)

Fig. 2 Comparison of immunoreactive score (IRS) classification of PSMA expression of prostate cancer primary tumor in lobes with focal and non-focal accumulation of [^{68}Ga]Ga-PSMA. IRS, 4-point immunoreactive score classification based on percentage of PSMA-positively stained cells and staining intensity. $p < 0.01$ (t -test)

The median TV of the PSMA-positive tumors was 5.4 mL (0.2–32.9) and thus significantly higher than the median TV of the PSMA-negative tumors (1.6 mL; 0.3–18.3, $p < 0.001$), respectively. Figure 3 illustrates that PET negativity occurs most frequently in small tumors (< 2 mL), whereas PET positive lesions were associated with larger tumor volumes.

The median percentage of PSMA-positively stained cells was significantly higher in PSMA-PET positive as

compared to PET-negative lobes (90% vs. 75%, range 5–100 vs. 20–100, respectively; $p = 0.01$). There was a significant but weak correlation between SUV_{max} and percentage of PSMA-positive tumor cells in all lobes ($r = 0.46$, $p < 0.001$; Fig. 4), with slightly higher correlation ($r = 0.52$, $p < 0.001$) only in PSMA-PET positive lobes. Applying a cutoff value of PSMA-positive cells $\geq 90\%$, 35/44 (~80%) lobes were positive in PSMA-PET imaging. On the other hand, 19/36 (~53%) lobes with $< 90\%$ PSMA-positive cells were PSMA-PET negative. An example of bilateral PCa showing focal uptake in one prostate lobe (with 90% PSMA-positive cells) and no focal uptake in the other lobe (50% PSMA-positive cells) is presented in Fig. 5. Figure 6 shows heterogeneity of PSMA expression, with areas of PSMA-negative PCa cells constituting about 10% of the primary tumor (GSC 7, ISUP 2, SUV_{max} 10.5, IRS 2).

In multivariate logistic regression analysis, only SUV_{max} proved as a significant factor predicting focal tracer uptake of [^{68}Ga]Ga-PSMA of PCa, with odds ratio 4.06 ($p = 0.001$), while TV and IRS were significant factors predicting focal accumulation only in univariate analyses, with odds ratios 1.23 ($p = 0.005$) and 3.086 ($p = 0.013$), respectively.

A summary of the characteristics of PSMA PET-positive and negative tumors is presented in Table 2. Median IRS classification for NP was 2 (1–3), IQR 2–2.

Lymph nodes

In 7 PSMA PET positive and 13 negative LNs, the median percentage of positively stained cells was 100 (40–100) vs. 100 (80–100), respectively ($p = 0.77$, Mann-Whitney

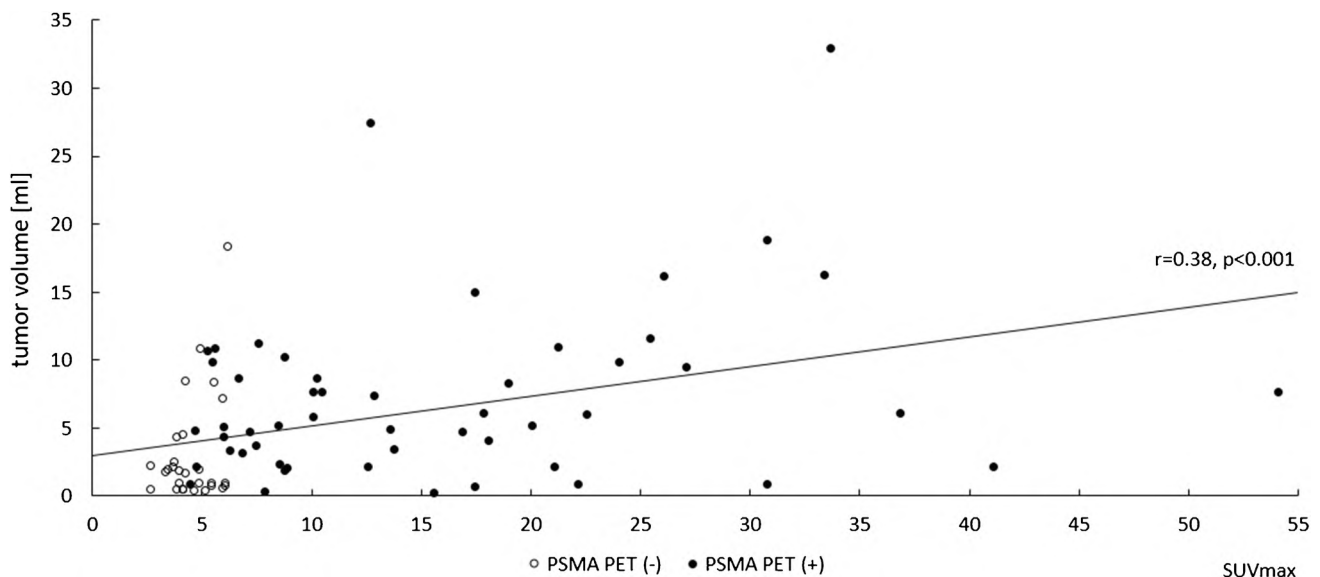


Fig. 3 Correlation of intensity of [^{68}Ga]Ga-PSMA uptake (SUV_{max}) in the primary tumor of prostate cancer with tumor volume in PSMA PET-positive (black dots) and -negative lobes (white dots)

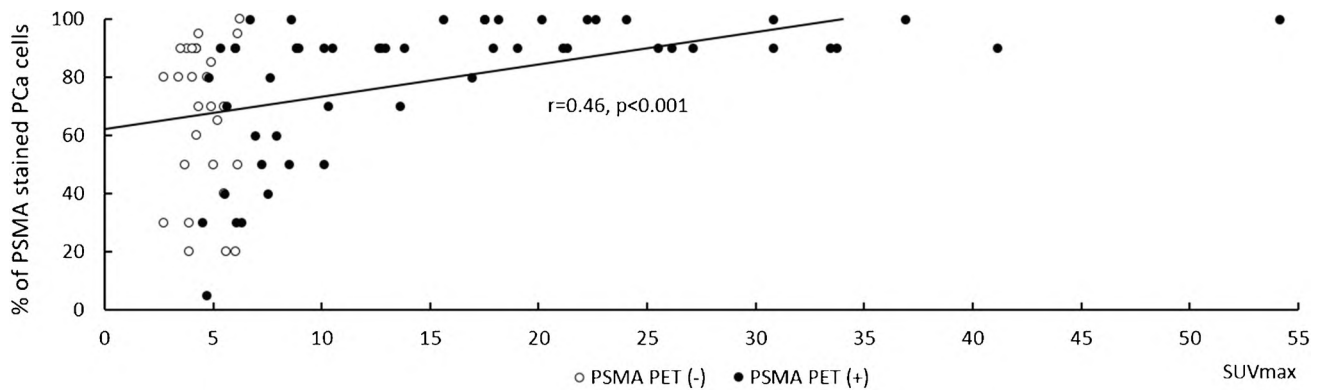


Fig. 4 Correlation of intensity of [^{68}Ga]Ga-PSMA uptake (SUV_{max}) in the primary tumor of prostate cancer with percentage of PSMA-positively stained cells in immunohistochemical validation, in PSMA PET-positive (black dots) and negative lobes (white dots)

U test), while the median intensity of staining was 3 (2–3) vs. 3 (3–3), respectively ($p = 0.80$, Mann-Whitney *U* test), thus without significant differences. Examples of LNs with focal and non-focal uptake are presented in Figs. 7 and 8, respectively. Furthermore, PSMA expression in metastatic LNs was significantly higher as compared

to corresponding primary tumors, with values of PSMA stained cells of 100% (40–100) vs. 90% (20–100), respectively ($p = 0.003$, Mann-Whitney *U* test) and a level of staining intensity of 3 (2–3), IQR 3–3 vs. 3 (2–3), IQR 2–3, respectively ($p = 0.024$, Mann-Whitney *U* test).

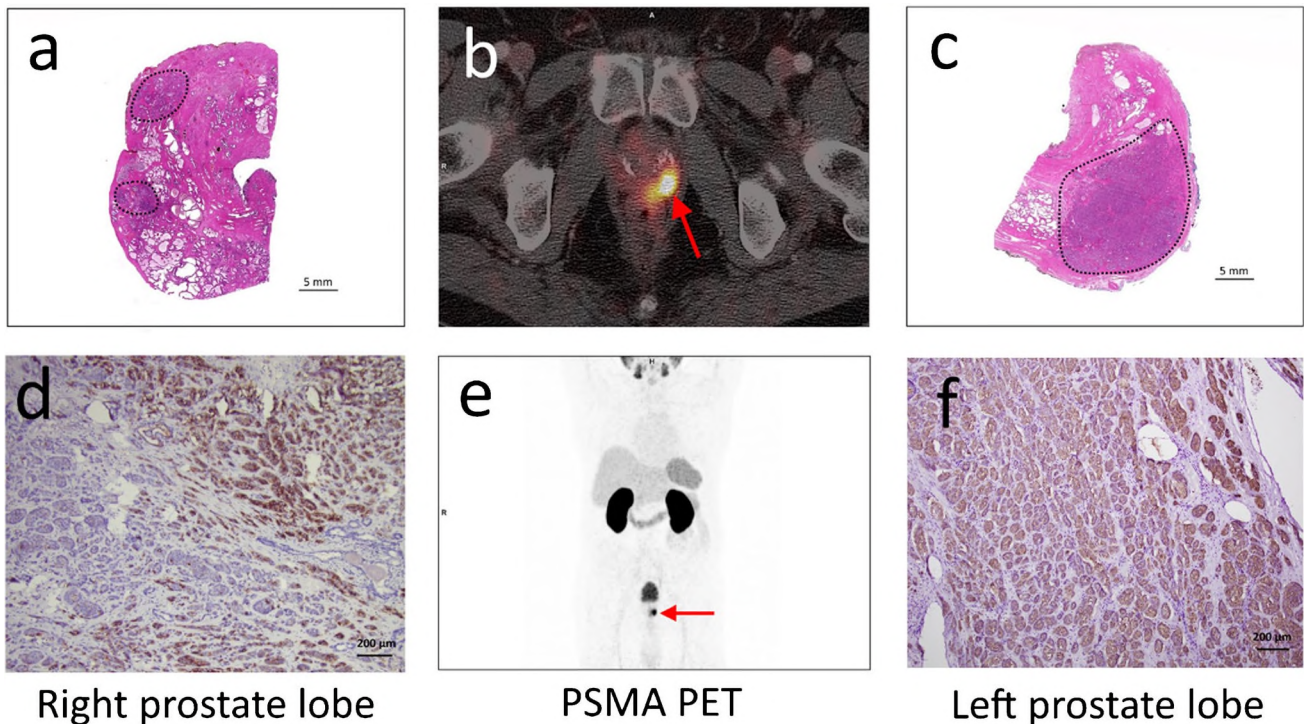
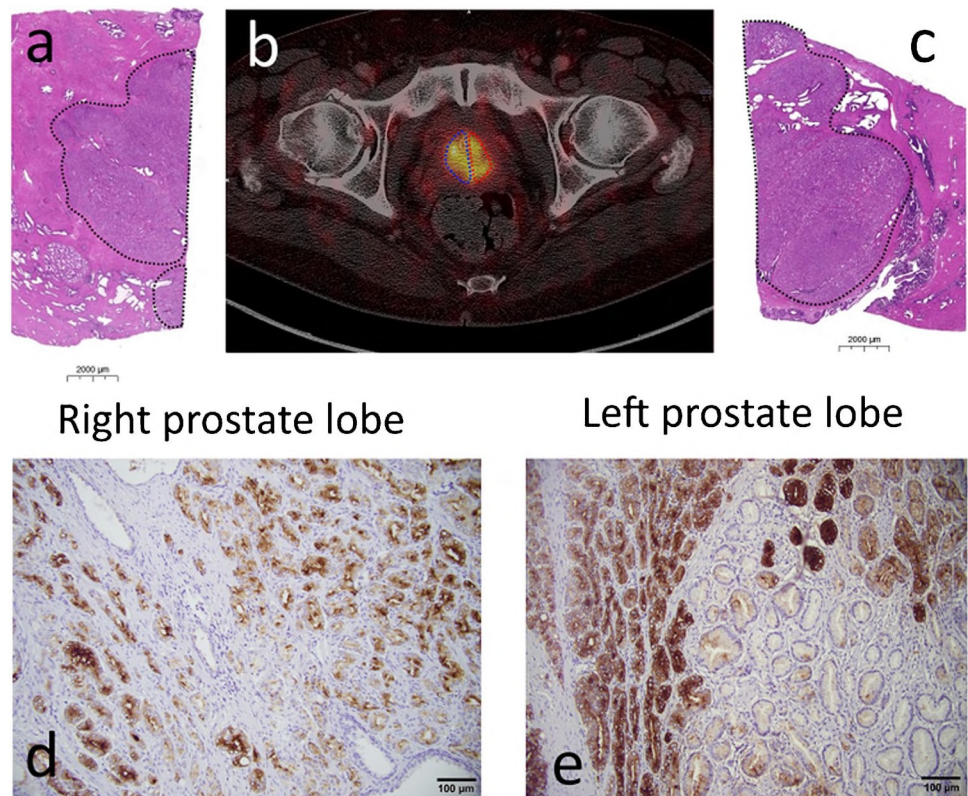


Fig. 5 55-year-old patient with high-risk prostate cancer, Gleason score 9, ISUP grade group 5, initial PSA 16 ng/mL. Pre-operative [^{68}Ga]Ga-PSMA PET/CT imaging (maximum intensity projection, MIP (e), fused PET/CT image showing axial cross-section of the prostate gland (b)) presenting focal tracer uptake in the left prostate lobe (SUV_{max} 41.1, red arrows) and non-focal accumulation in the right prostate lobe (SUV_{max} 3.7). In both lobes, post-operative

H&E staining confirmed the presence of PCa involving 10–15% of the lobes' volume (delineated by black dashed line (a, c)). In the left lobe, the tumor presented high and homogenous PSMA expression in 90% of PCa cells, IRS 3 (f), whereas in the right lobe, the tumor presented as dispersed islands of cancerous tissue of moderate (IRS 2) and heterogeneous (~50%) PSMA expression (d). Tumor volume in each lobe was 2.1 mL

Fig. 6 Heterogeneity of PSMA expression in the primary tumor of prostate cancer revealed in immunohistochemical PSMA validation. Infiltration of both prostate lobes (GSC 7, ISUP 2, (a, c)) presenting PSMA-positive (SUV_{max} 10.5 in right lobe; SUV_{max} 10.1 in left lobe) in the pre-operative [^{68}Ga]Ga-PSMA PET/CT (cross-sectional image, tumor in the right lobe delineated by blue dashed line, in the left lobe — by red dashed line, (b)). In both lobes among positively stained cells (IRS 2), occasionally areas of PSMA-negative cells, constituting ~10% of the tumor (d, e). Tumor volume in each lobe was 7.6 mL



Focal uptake in [^{68}Ga]Ga-PSMA PET/CT and extra-prostatic disease

Among 33 patients presenting focal uptake in at least one prostatic lobe, 33% (11/33) had LNM detected in

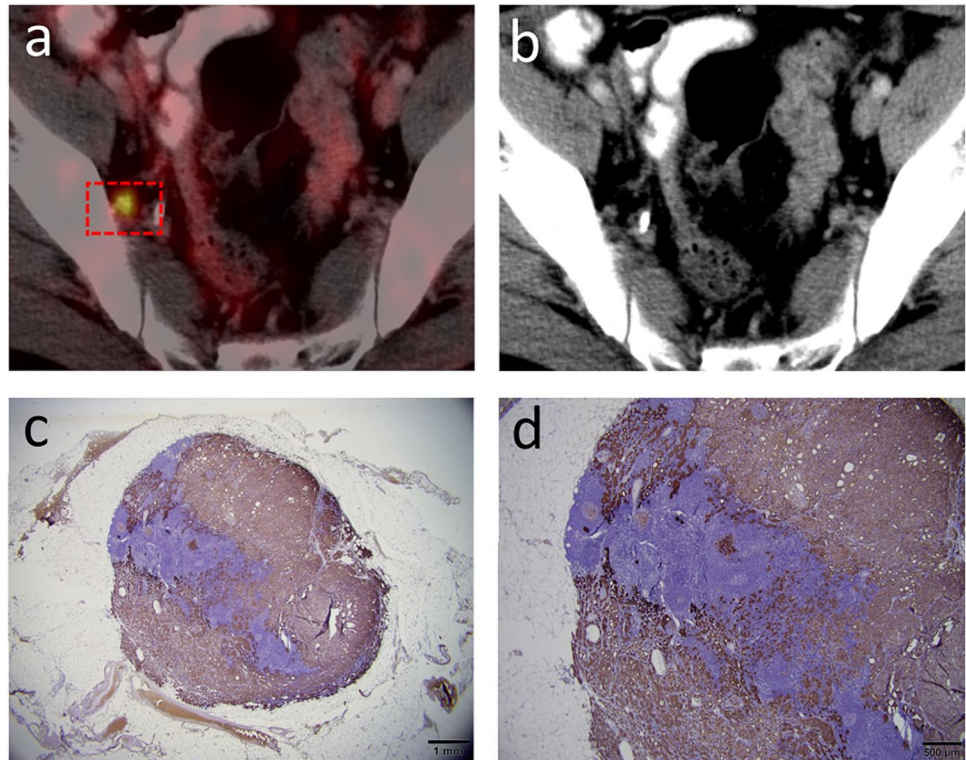
post-operative histopathology, while in the remaining 7 PSMA-negative patients, only 1 had regional LN involvement. As far as M+ disease is concerned, PSMA-avid distant lesions, predominantly in bones, were observed in 15% (5/33) and 0% (0/7) of patients with PSMA-positive and

Table 2 Comparison of various parameters of primary tumors of prostate cancer in PSMA-positive and -negative lobes in the pre-operative PET/CT imaging

Parameter	PSMA PET (+) tumors	PSMA PET (–) tumors	<i>p</i> -value, statistical test
Median SUV_{max}	12.8 (4.5–54.1)	4.3 (2.7–6.2)	$p < 0.001$, K-W test*
Median GSC	7 (7–10), IQR 7–9	7 (7–10), IQR 7–7	$p = 0.03$, M-W <i>U</i> test**
Mean GSC	7.9 ± 1.0	7.3 ± 0.8	
D’Amico risk group	39% (13/33) pts with intermediate, 61% (20/33) pts with high-risk PCa	100% (7/7) pts with intermediate-risk PCa	
Median ISUP grade group	3 (2–5)	3 (2–3)	$p = 0.07$, M-W <i>U</i> test**
Median PSA level (ng/mL)	12.2 (3.7–140.0)	5.8 (1.6–10.7)	$p = 0.002$, M-W <i>U</i> test**
Median PSA density (ng/mL ²)	0.4 (0.1–2.6)	0.2 (0.02–0.3)	$p = 0.01$, M-W <i>U</i> test**
Median IRS (0–12)	8 (3–12), IQR 6–12	7 (2–12), IQR 4–8	$p = 0.02$, M-W <i>U</i> test**
Median IRS classification (PSMA expression)	2 (1–3), IQR 2–3	2 (1–3), IQR 2–2	$p = 0.04$, M-W <i>U</i> test**
Median tumor volume (mL)	5.4 (0.2–32.9), IQR 2.7–9.8	1.6 (0.3–18.3), IQR 0.6–3.3	$p < 0.001$, M-W <i>U</i> test**
Median percentage of PSMA positively stained cells (%)	90 (5–100), IQR 70–95	75.0 (20–100), IQR 50–90	$p = 0.01$, M-W <i>U</i> test**

*K-W test, Kruskal-Wallis test; **M-W *U* test, Mann-Whitney *U* test; IQR, interquartile range; GSC, Gleason score; PCa, prostate cancer; ISUP, International Society of Urological Pathologists; PSA, prostate-specific antigen; IRS, immunoreactive score; PSMA, prostate-specific membrane antigen

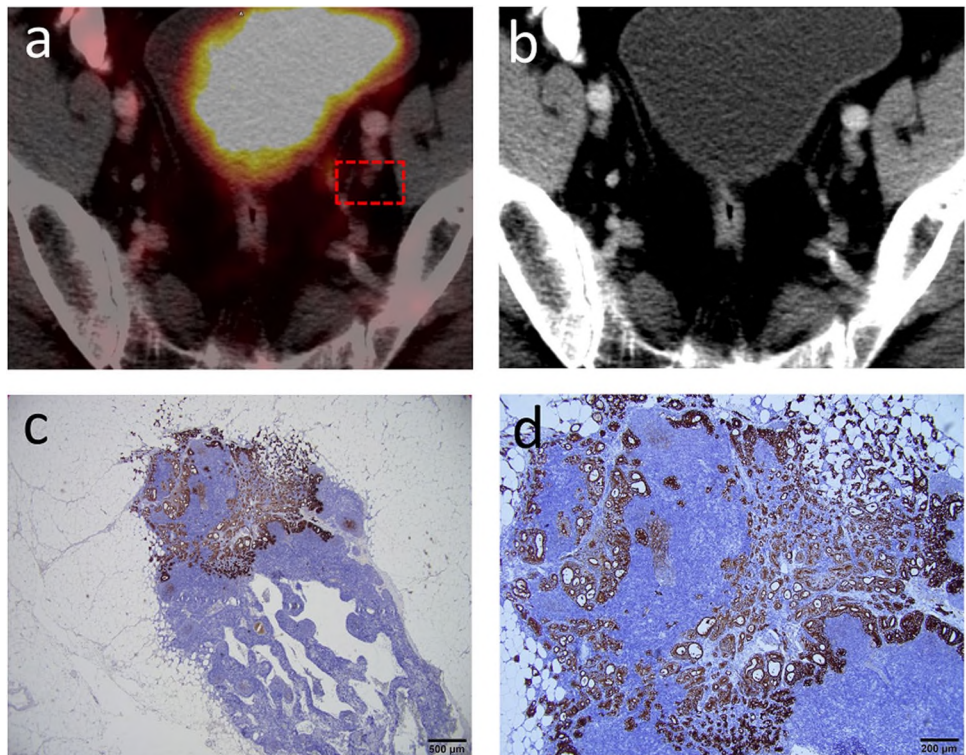
Fig. 7 An example of 53-year-old patient with high-risk prostate cancer, Gleason score 8, ISUP grade group 4, initial PSA 34.6 ng/mL. Pre-operative [^{68}Ga]Ga-PSMA PET/CT imaging (fused PET/CT image (a); CT image, axial cross-sections (b)) presenting focal tracer uptake in the right obturator lymph node (SUV_{max} 6.7, outlined by red dashed rectangle) harboring 7-mm metastasis, with 100% of cancer cells showing intense PSMA staining in immunohistochemical validation (c, d)



-negative primary tumors, respectively. The PSMA-positive group was dominated by high-risk PCa (61%, 20/33), while the PSMA-negative group contained only patients

with intermediate-risk disease, according to D'Amico classification.

Fig. 8 An example of 57-year-old patient with high-risk prostate cancer, Gleason score 7, ISUP grade group 3, initial PSA 60.6 ng/mL. Immunohistochemical validation (c, d) revealed the presence of 2mm micrometastasis in the left obturator lymph node with intense PSMA staining in 100% of cancer cells and no focal tracer uptake at pre-operative [^{68}Ga]Ga-PSMA PET/CT imaging (fused PET/CT image, outlined by red dashed rectangle (a); CT image, axial cross-sections (b))



Focal uptake in [^{68}Ga]Ga-PSMA PET/CT and serum PSA-values

The median PSA-level in patients with PSMA-positive primary tumors was 12.2 ng/mL (3.7–140.0) vs. 5.8 (1.6–10.7) in PSMA-negative patients ($p = 0.002$, Mann-Whitney U test); also, statistically significant difference was reported in case of PSA density (defined as total PSA divided by prostate volume) — the median PSA density was 0.4 ng/mL² (0.1–2.6) vs. 0.2 (0.02–0.3) for PSMA-positive and -negative tumors, respectively ($p = 0.01$, Mann-Whitney U test).

Survival

In 27 patients, follow-up data were available. At a median follow-up of 7 (range 1–46) months, 67.1% (18/27) patients were free from disease progression after radical treatment. In the Kaplan-Meier survival analysis, PFS significantly correlated with PSMA PET status at pre-operative imaging, with lower risk of progression in patients with negative PSMA-PET ($p = 0.04$, Cox's F test, Fig. 9).

Discussion

PSMA PET imaging is a superior tool in the management of prostate cancer patients as it has the highest accuracy in detecting disease foci at different stages of disease [16, 17]. However, up to 20% of patients do not overexpress PSMA on their PCa cells, which makes PSMA PET unreliable in this sub-cohort [5]. In our study, 83% of patients presented

with focal uptake in at least one prostate lobe of their primary tumors. Of note, the PSMA-negative patients were less frequently diagnosed with high risk PCa (according to D'Amico classification), had no distant metastases, and had lower risk of disease progression after radical treatment in the Kaplan-Meier survival analysis. This observation is in line with the results of a study by Hupe et al., who also showed that the likelihood of disease recurrence is associated with increased PSMA expression in tumor tissue [18]. Thus, PSMA expression in the primary tumor as identified non-invasively by PET may correlate positively with the aggressiveness of PCa. Therefore, the result of PSMA PET pre-operative imaging could be regarded as an important factor in risk calculators and nomograms to provide optimal therapy while minimizing overtreatment in clinically localized disease [19]. This potentially clinically relevant information should be verified in larger patient cohorts.

Several factors could be potential reasons for PSMA-negativity at imaging. First of all, tumor volume — most of the PSMA-negative tumors in our study — had a volume below 2.0 mL, which could substantially underestimate uptake values due to the so called partial volume effect (PVE) [15]. Apart from the tumor size, also organ movement, involving prostate as well, could introduce a blurring effect that results in additional PVE. Secondly, an important role plays intratumoral heterogeneity with PSMA-negative tumor cells. The intensity of tracer uptake (expressed as SUV_{max}) correlates to a certain extent with the percentage of PSMA stained cells ($r = 0.46$, $p < 0.001$) and the level of PSMA expression validated immunohistochemically. However, the differences of IRS classification between PSMA PET-positive and -negative tumors were moderate, with some degree of overlap. Hence, neither TV nor IRS was an independent factor predicting focal uptake of [^{68}Ga]Ga-PSMA. Thirdly, the tumor grade expressed by GSC significantly differed in PSMA PET-positive and -negative lobes, again with certain degree of overlap. Finally, potential artifacts in the process of histological preparation could take place, with the 4- μm specimen slices being not fully representative.

Among the potential reasons for a negative PSMA PET scan one should also mention neuroendocrine differentiation, as presented in the paper by Fendler et al. [20]. PSMA gene (*FOLH1*) expression was shown to inversely correlate with the markers of neuroendocrine differentiation, such as overexpression of NSE (neuron-specific enolase) and SSTR2 (somatostatin receptor 2) in a pre-clinical analysis performed by Bakht et al. [21]. However, in our cohort, we could not identify that subtype of PCa in any of the specimens.

A certain level of heterogeneity of PSMA expression was observed in the majority of our patients (in only 18%, 14/80 lobes, the percentage of positively stained cells was 100%). This observation may suggest that heterogeneity of PSMA expression is a common feature of prostate cancer, which

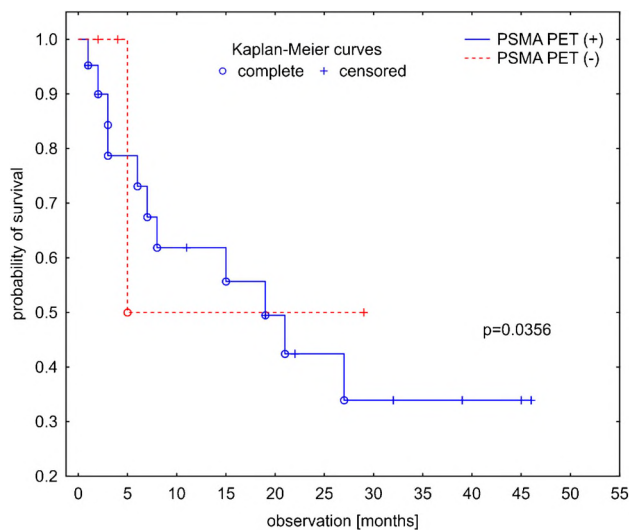


Fig. 9 Kaplan-Meier progression free survival estimates for prostate cancer patients treated with curative intent, depending on the presence of focal uptake of [^{68}Ga]Ga-PSMA in the primary tumor at pre-operative PET/CT

would be consistent with the paper by Mannweiler et al. [22] based exclusively on microscopic evaluation. The authors observed large areas with PSMA-negative cells, which was the case in our cohort, as well. However, uniformly negative cases are rare — Mannweiler et al. found one such primary tumor (and metastasis) among 50 cases, while we did not find any. It should also be emphasized that from the histopathological point of view, both in our material and in the above quoted paper, no characteristic morphological features of PSMA PET-negative tumors were found.

In the recently published paper by Rüschoff et al. [23], the authors observed different growth patterns of PSMA-positive and negative tumors. We think that due to multifocal growth of PCa at certain time point, most of the tumors will present as expansive mass of pure carcinoma glands replacing normal glands; therefore, from this point of view, the differences seem to be more quantitative and relate to the extent of tumor involvement. Rüschoff et al. proposed a threshold of $\geq 20\%$ PSMA-negative cell at IHC as the optimal cutoff for negative versus positive scans. Our data suggest that this value might be even lower ($< 10\%$), since we observed that tumors with $\geq 90\%$ PSMA-positive cells were positive at PET imaging in $\sim 80\%$.

The results of our study also seem to somewhat differ from those presented by Woythal et al. [2]. The authors reported high and homogenous expression of PSMA in PCa with only low levels of PSMA expression in NP, while in our study, there were patients with a wide range of heterogeneity in PSMA expression, both with focal and non-focal tracer uptake, while in NP, the median IRS classification was 2 (1–3), IQR 2–2.

A possible explanations of relatively high PSMA expression in PET negative cases or even in NP is the potential availability of a cytoplasmic PSMA variant released from dead cells during IHC validation, which is not accessible for *in vivo* agents. This phenomenon might be an important limiting factor in the use of IHC as the gold standard for assessing PSMA expression. In addition, the PSMA upregulation could take place between PET imaging and prostatectomy, as a result of the action of various biological factors and the tumor microenvironment.

Regarding the LN analysis, in PSMA PET-positive and -negative LNs, the percentage and intensity of staining were high and almost equal, with no significant differences; therefore, we argue that the volume of metastatic tissue within a LN and not PSMA expression is crucial for detectability at PET imaging. We showed a significant difference of intranodal size of these metastases in PSMA PET-positive and -negative nodes in our previous study [9] (median size of 10 mm, range 1.5–17 vs. 4 mm, range 1–9, respectively, $p = 0.008$, Mann-Whitney U test). In the current study, we also show higher PSMA expression in LN metastases as compared to the respective primary tumors. These results

are consistent with the study by Ferraro et al. [24], which described uniform PSMA expression in a metastatic LN originating from a heterogeneous primary tumor (60% of PSMA-negative cancer cells). The authors compared PSMA-PET detection rates in the biochemical relapse setting depending on the PSMA expression patterns of primary tumor. These observations highlight the differences in PSMA expression of the primary lesion and its lymph node metastases and are a further evidence of the high metastatic potential of PSMA-positive PCa cells.

The novel aspect of this study is also the fact that a different molecule (PSMA I&T) was used for imaging compared to other studies (PSMA-11). Our compound is used not only for imaging but also for therapy; therefore, PSMA I&T PET also identifies potential therapeutic targets and may predict response to therapy. To the best of our knowledge, this is the first study to show histopathologic cross-referencing for PSMA I&T.

Limitations of our study include its retrospective and single-center nature and relatively small number of patients.

Conclusion

Positive [^{68}Ga]Ga-PSMA PET/CT scan of primary tumor of PCa results from a combination of factors, such as homogeneity and intensity of PSMA expression, tumor volume and grade, with a cutoff value of $\geq 90\%$ PSMA-positive cells strongly determining PET-positivity. Focal accumulation of [^{68}Ga]Ga-PSMA in the primary tumor may correlate positively with aggressiveness of prostate cancer, harboring higher risk of regional lymph node involvement and distant metastatic spread, and may be associated with worse prognosis.

Author contribution Andreas K. Buck contributed to the study conception and design. Material preparation, data collection, and analysis were performed by Wojciech Cytawa, Stefan Kircher, Simon Weber, Philipp Hartrampf, Tomasz Bandurski, Constantin Lapa, and Anna Katharina Seitz. The first draft of the manuscript was written by Wojciech Cytawa. Writing — review and editing were performed by Wojciech Cytawa, Stefan Kircher, Constantin Lapa, Anna Katharina Seitz, and Andreas K. Buck. All authors read the manuscript, commented on it, and approved its final version.

Data availability The datasets generated during and/or analyzed during the current study are available from the corresponding author on reasonable request.

Declarations

Ethics approval All procedures involving human participants were in accordance with the ethical standards of the institutional and/or national research committee and with the 1964 Helsinki Declaration and its later amendments or comparable ethical standards.


Consent to participate Informed consent was obtained from all individual participants included in the study.

Conflict of interest Hans-Jürgen Wester is the founder and shareholder of Scintomics. All other authors have no relevant financial or non-financial interests to disclose.

References

- Sung H, Ferlay J, Siegel RL, et al. Global cancer statistics 2020: GLOBOCAN estimates of incidence and mortality worldwide for 36 cancers in 185 countries. *CA Cancer J Clin*. 2021;71(3):209–49. <https://doi.org/10.3322/caac.21660>.
- Woythal N, Arsenic R, Kempkensteffen C, et al. Immunohistochemical Validation of PSMA expression measured by (68)Ga-PSMA PET/CT in primary prostate cancer. *J Nucl Med*. 2018;59:238–43. <https://doi.org/10.2967/jnumed.117.195172>.
- Afshar-Oromieh A, Malcher A, Eder M, et al. PET imaging with a [68Ga]gallium-labelled PSMA ligand for the diagnosis of prostate cancer: biodistribution in humans and first evaluation of tumour lesions. *Eur J Nucl Med Mol Imaging*. 2013;40:486–95. <https://doi.org/10.1007/s00259-012-2298-2>.
- Corfield J, Perera M, Bolton D, et al. (68)Ga-prostate specific membrane antigen (PSMA) positron emission tomography (PET) for primary staging of high-risk prostate cancer: a systematic review. *World J Urol*. 2018;36:519–27. <https://doi.org/10.1007/s00345-018-2182-1>.
- Emmett L, Willows K, Violet J, et al. Lutetium (177) PSMA radionuclide therapy for men with prostate cancer: a review of the current literature and discussion of practical aspects of therapy. *J Med Radiat Sci*. 2017;64:52–60. <https://doi.org/10.1002/jmrs.227>.
- Afshar-Oromieh A, Babich JW, Kratochwil C, et al. The rise of PSMA ligands for diagnosis and therapy of prostate cancer. *J Nucl Med*. 2016;57:79S–89S. <https://doi.org/10.2967/jnumed.115.170720>.
- D'Amico AV, Whittington R, Malkowicz SB, et al. Biochemical outcome after radical prostatectomy, external beam radiation therapy, or interstitial radiation therapy for clinically localized prostate cancer. *JAMA*. 1998;280:969–74. <https://doi.org/10.1001/jama.280.11.969>.
- Mottet N, Bellmunt J, Bolla M, et al. EAU-ESTRO-SIOG guidelines on prostate cancer. Part 1: Screening, Diagnosis, and Local Treatment with Curative Intent. *Eur Urol*. 2017;71:618–629. <https://doi.org/10.1016/j.eururo.2016.08.003>.
- Cytawa W, Seitz AK, Kircher S, et al. 68Ga-PSMA I&T PET/CT for primary staging of prostate cancer. *Eur J Nucl Med Mol Imaging*. 2020;47:168–77. <https://doi.org/10.1007/s00259-019-04524-z>.
- Kaemmerer D, Peter L, Lupp A, et al. Molecular imaging with ⁶⁸Ga-SSTR PET/CT and correlation to immunohistochemistry of somatostatin receptors in neuroendocrine tumours. *Eur J Nucl Med Mol Imaging*. 2011;38:1659–68. <https://doi.org/10.1007/s00259-011-1846-5>.
- Sheikhabaei S, Afshar-Oromieh A, Eiber M, et al. Pearls and pitfalls in clinical interpretation of prostate-specific membrane antigen (PSMA)-targeted PET imaging. *Eur J Nucl Med Mol Imaging*. 2017;44:2117–36. <https://doi.org/10.1007/s00259-017-3780-7>.
- Rowe SP, Pienta KJ, Pomper MG, et al. Proposal for a structured reporting system for prostate-specific membrane antigen-targeted PET imaging: PSMA-RADS version 1.0. *J Nucl Med*. 2018;59:479–485. <https://doi.org/10.2967/jnumed.117.195255>.
- Eiber M, Herrmann K, Calais J, et al. Prostate cancer molecular imaging standardized evaluation (PROMISE): proposed miTNM classification for the interpretation of PSMA-ligand PET/CT. *J Nucl Med*. 2018;59:469–79. <https://doi.org/10.2967/jnumed.117.198119>.
- Murciano-Goroff YR, Wolfsberger LD, Parekh A, et al. Variability in MRI vs. ultrasound measures of prostate volume and its impact on treatment recommendations for favorable-risk prostate cancer patients: a case series. *Radiat Oncol*. 2014;9:200. <https://doi.org/10.1186/1748-717X-9-200>.
- Soret M, Bacharach SL, Buvat I. Partial-volume effect in PET tumor imaging. *J Nucl Med*. 2007;48:932–45. <https://doi.org/10.2967/jnumed.106.035774>.
- Perera M, Papa N, Christidis D, et al. Sensitivity, specificity, and predictors of positive 68Ga-prostate-specific membrane antigen positron emission tomography in advanced prostate cancer: a systematic review and meta-analysis. *Eur Urol*. 2016;70:926–37. <https://doi.org/10.1016/j.eururo.2016.06.021>.
- Hofman MS, Lawrentschuk N, Francis RJ, et al. Prostate-specific membrane antigen PET-CT in patients with high-risk prostate cancer before curative-intent surgery or radiotherapy (proPSMA): a prospective, randomised, multicentre study. *Lancet*. 2020;395:1208–16. [https://doi.org/10.1016/S0140-6736\(20\)30314-7](https://doi.org/10.1016/S0140-6736(20)30314-7).
- Hupei MC, Philippi C, Roth D, et al. Expression of prostate-specific membrane antigen (PSMA) on biopsies is an independent risk stratifier of prostate cancer patients at time of initial diagnosis. *Front Oncol*. 2018;8:623. <https://doi.org/10.3389/fonc.2018.00623>.
- Hanna B, Ranasinghe W, Lawrentschuk N. Risk stratification and avoiding overtreatment in localized prostate cancer. *Curr Opin Urol*. 2019;29:612–9. <https://doi.org/10.1097/MOU.0000000000000672>.
- Fendler WP, Schmidt DF, Wenter V et al. 68Ga-PSMA PET/CT detects the location and extent of primary prostate cancer. *J Nucl Med*. 2016; 57:1720–1725. <https://doi.org/10.2967/jnumed.116.172627>.
- Bakht MK, Derecichei I, Li Y et al. Neuroendocrine differentiation of prostate cancer leads to PSMA suppression. *Endocr Relat Cancer*. 2018; 26:131–146. <https://doi.org/10.1530/ERC-18-0226>.
- Mannweiler S, Amersdorfer P, Trajanoski S, et al. Heterogeneity of prostate-specific membrane antigen (PSMA) expression in prostate carcinoma with distant metastasis. *Pathol Oncol Res*. 2009;15:167–72. <https://doi.org/10.1007/s12253-008-9104-2>.
- Rüschhoff JH, Ferraro DA, Muehlematter UJ, et al. What's behind 68 Ga-PSMA-11 uptake in primary prostate cancer PET? Investigation of histopathological parameters and immunohistochemical PSMA expression patterns. *Eur J Nucl Med Mol Imaging*. 2021;48:4042–53. <https://doi.org/10.1007/s00259-021-05501-1>.
- Ferraro DA, Rüschhoff JH, Muehlematter UJ et al. Immunohistochemical PSMA expression patterns of primary prostate cancer tissue are associated with the detection rate of biochemical recurrence with 68Ga-PSMA-11-PET. *Theranostics*. 2020; 10: 6082–6094. <https://doi.org/10.7150/thno.44584>.

Authors and Affiliations

Wojciech Cytawa^{1,2}  · Stefan Kircher³ · Hubert Kübler⁴ · Rudolf A. Werner¹ · Simon Weber¹ · Philipp Hartrampf¹ · Tomasz Bandurski⁵ · Piotr Lass² · Wojciech Połom⁶ · Marcin Matuszewski⁶ · Hans-Jürgen Wester⁷ · Constantin Lapa⁸ · Andreas Rosenwald³ · Anna Katharina Seitz⁴ · Andreas K. Buck¹

¹ Department of Nuclear Medicine, University Hospital Würzburg, Würzburg, Germany

² Department of Nuclear Medicine, Medical University of Gdańsk, Smoluchowskiego Str. 17, 80-952, Gdańsk, Poland

³ Institute of Pathology, Comprehensive Cancer Center Mainfranken (CCCMF), University of Würzburg, Würzburg, Germany

⁴ Department of Urology, University Hospital Würzburg, Würzburg, Germany

⁵ Department of Radiology Informatics and Statistics, Medical University of Gdańsk, Gdańsk, Poland

⁶ Department of Urology, Medical University of Gdansk, Gdańsk, Poland

⁷ Pharmaceutical Radiochemistry, Technische Universität München, Munich, Germany

⁸ Nuclear Medicine, Medical Faculty, University of Augsburg, Augsburg, Germany